韓國鑛物學會誌 第 4 卷 第 1 號(1991)
J. Miner. Soc. Korea, 4, 11－21(1991)

One-dimensional XRD-Pattern Calculations of Clay Minerals I. Dioctahedral and Trioctahedral Fe-rich Smectites

粘土鑛物의一次元的 X-線 回折圖形의 計算: I. Dioctahedral 과 Trioctahedral Fe-rich 스멕타이트

Jung Ho Ahn (안 중 호)

Marine Mineral Resources Laboratory, Korea Ocean Research and Development Institute, Ansan 425－600, Korea.
(韓國海洋硏究所)

ABSTRACT: XRD patterns of beidellite-nontronite and saponite-iron saponite series were investigated using one-dimensional pattern simulation method. Ethylene-glycolated smectites show stronger 002 and 003 reflections than hydrated specimens do. The intensities of the 002 and 003 reflections change systematically as a function of Fe enrichment in both types of smectites. The intensity ratio of 002/003 increases with increasing Fe in both dioctahedral and trioctahedral smectites that are ethylene-glycolated. Such intensity change is attributed to the higher scattering factor of Fe than those of Al and Mg, and the scattering power of various smectites can be compared quantitatively by calculating the scattering factors of octahedral cations. Interlayer cations cause less effect on XRD profile than octahedral cations as Fe do. Although 00*l* reflections provide informations about the overall scattering power of the octahedral sheet, some ferrous dioctahedral smectite cannot be distinguished unambiguously from trioctahedral smectites on the basis of XRD profile.

Simulation showed that heterogeneous smectites exhibit 00*l* intensity distribution that is almost identical to that of homogeneous smectites having the average composition of heterogeneous ones. The broadening of 00*l* reflections may not be useful in evaluating the degree of heterogeneity of smectite unless other factors affecting the broadening are well known.

요약: 1차원적 X-선 회절도형의 계산방법을 이용하여 Beidellite-nontronite 와 saponite-iron saponite 의 X-선 회절현상을 조사하였다. 에틸렌 글리콜 처리된 스멕타이트는 수화된 스멕타이트보다 강한 002 와 003 회절선을 나타내는데, 002 와 003 회절선은 Fe 성분의 함량에 따라서 그 강도가 점진적으로 변화한다. 에틸렌 글리콜처리된 dioctahedral 스멕타이트와 trioctahedral 스멕타이트에서 002/003 회절선 강도비율은 스멕타이트내에 Fe 성분이 많아짐에 따라 높아진다. 이러한 비율의 변화는 Al 이나 Mg 보다 훨씬높은 Fe 의 scattering factor 에 기인한 것이며, octahedral 양이온들의 scattering factor 들을 계산함으로서 여러 스멕타이트들의 X-선 회절선들을 정량적으로 비교할 수 있다. Interlayer 양이온들은 Fe 등의 octahedral 양이온들에 비해서 X-선 회절선들에 경미한 영향을 미친다. 00*l* 회절선들이 octahedral sheet 의 전반적인 회절선강도에 관한 자료를 제공하지만, Fe 성분이 많은 일부 dioctahedral 스멕타이트들은 1차원적 X-선 회절도형만으로는 trioctahedral 스멕타이트로부터 명확하게 구분될 수 없다.

1차원적 X-선 회절도형의 계산에 의하면 복합체로 이루어진 이질의 스멕타이트의 00*l* 회절선 분포양상은 이 이질의 스멕타이트 화학성분의 평균 성분에 해당하는 균질 스멕타이트와 거의 같다. 회절선이 넓어지는 현상에 관련된 여러 요소들이 잘 파악되지 않으면, 00*l* 회절선들이 넓어지는 정도를 스멕타이트의 이질도를 판단하기 위해 응용하는 데는 문제점이 있는 것으로 사료된다.

INTRODUCTION

Clay minerals have wide range of structures and chemistry, and they constitute various mixed-layered crystals. Powder X-ray diffraction (XRD) is most widely used in characterizing and studying clay minerals because of relatively easy access to powder X-ray diffractometers and fine particle size of clay minerals. Calculated one-dimensional XRD patterns are useful in interpreting and analyzing experimental XRD patterns; simulated XRD patterns can be calculated based on model structures and experimental conditions, and simulated XRD patterns can be compared with experimental ones. The effect of structural variation, chemistry, crystal size, and mixed layering on XRD profile can be investigated by calculating XRD patterns.

Simulated diffraction patterns of clays have been produced successfully by calculation method using computer. Reynolds (1967) and Reynolds and Hower (1970) introduced one-dimensional XRD patterns of mixed-layer illite/smectite (I/S), and their result showed that ordering type and proportion of illite and smectite in mixed-layer I/S can be accurately determined by comparing experimental XRD patterns with calculated patterns. Since the work by Reynolds and Hower (1970), XRD pattern calculation was vigorously used by many investigatiors in interpreting XRD patterns of actual mixed-layer clay minerals (e.g., Perry and Hower, 1970; Hower et al., 1976; Nadeau et al., 1984a, 1984b; Altaner and Bethke, 1988).

The composition of smectite is in wide range depending on its occurrence. Dioctahedral smectites such as montmorillonite are most abundant among smectite, and they commonly occur as a constituent of mixed-layer I/S in pelitic and hydrothermally altered rocks and in unmetamorphosed bentonites. Nontronite and trioctahedral Fe-rich smectite are the predominant authegenic clay minerals in deep-sea sediments, and they also occur in basalts altered by seawater and hydrothermal fluids (Güven, 1988).

Characterization of dioctahedral and trioctahedral smectites and estimation of approximate chemical composition from XRD patterns are complicated, although smectite can be easily identified by comparing XRD patterns of air-dried and ethylene glycol-solvated specimens. 00*l* reflections of smectite are closely related to the total scattering power of the octahedral layer, and therefore those reflections can be used in obtaining information about the chemistry of octahedral sheet such as the substitution of Fe in octahedral sites. The relationship between composition and 00*l* reflections of dioctahedral and trioctahedral smectites is in investigated in this study by utilizing XRD pattern calculation method.

Another intriguing problem in studying clays occurs when there is chemical and structural heterogeneity from crystal to crystal or even at unit-cell scale in investigated samples (Drits, 1987). Transmission electron microscopy (TEM) studies of clay minerals by Ahn and Peacor (1986) and Ahn and Buseck (1990) suggest that there may be chemical and structural variation even at a unit-cell scale. Soil or sediment samples may contain mixtures of smectites having various composition that are derived during transportation and deposition, but the mixtures of such smectites cannot be separated physically for XRD or chemical analyses. The effect of chemical heterogeneity of smectite on XRD profile was also examined by using simulated XRD patterns.

XRD PATTERN CALCULATION PROGRAM

X-ray diffraction intensities of smectites were simulated using the Macintosh version of the NEWMOD program (Reynolds, 1985). The NEWMOD program is based on the same basic theory as the previous MOD-series programs that are described by Reynolds and Hower (1970) and Reynolds (1980). The NEWMOD program is strengthened by adding a recursive routine which computes the statistical matrices (Bethke and Reynolds, 1986).

The number of Al atoms per four tetrahedral sites of the model structures are 0 and 0.35 for dioctahedral and trioctahedral smectites, respectively. Ca was assumed to be the interlayer cation for both types of smectites. The structure of

Table 1. Instrumental variables used in XRD pattern calculation.

Wavelength of X-ray	1.5418 Å
Divergence slit	1.0 degree
Goniometer radius	20 cm
Soller slit 1 (incident beam slit)	1 degree
Soller slit 2 (diffracted beam slit)	2 degree
Sample length	3.6 cm
θ compensationg slit	0

Table 2. Chemical and structural variables of samples used in XRD pattern calculation.

Exchange capacity	0.36
Exchange cation	Ca
Interlayer complex	2-glycol layers or 1-water layer
μ^*(mean sample mass absorption coefficient)	45
σ^*(standard deviation of the orientation function)	12
Low N	3
High N	14

Table 3. Structure for ethylene-glycolated smectite (from Reynolds, 1965).

Atoms	Atomic positions in Z(Å)
Al, Fe, Mg	0
O, OH	1.06
Si, Al	2.70
O	3.27
H_2C-HO	6.12
CH_2-OH	6.07
H_2O, Ca	7.94

two-layer ethylene glycol is from Reynolds (1965)(Table 1), and the one-layer water structure was assumed that water molecules are located at the center of the interlayer of smectite. Atomic scattering factors are calculated based on the method by Wright (1973). Half ionized atomic scattering factors are used for Si, Al, O, and H of the 2:1 layer structure, and fully ionized values are used for Mg, Fe, and Ca. Neutral atomic scattering factors are used for C, N, O, and H of ethylene glycol and water at the interlayer.

The modeling of the program assumes that crystals are oriented along the basal plane so only 00*l* reflections are produced. The basal spacings of 16.9 and 12.4Å were used for ethylene-glycolated and hydrated one-layer water smectites, respectively. The NEWMOD program is made for the calculation of XRD patterns of mixed-layer clays, and therefore two identical smectite components are assumed to be randomly interstratified (R = 0) in 50:50 proportion in order to calculate patterns of monomineralic smectites. Instrumental parameters and structural variables used in the calculations are in Tables 2 and 3.

XRD PATTERN CALCULATION RESULTS

Dioctahedral Smectites (Beidellite-Nontronite Series)

The diffraction patterns of Fig. 1 illustrate the effects of Fe content in ethylene-glycolated dioctahedral smectites. The 00*l* reflections in the patterns of smectites remain very strong regardless of the chemical changes. The intensities of the 002 and 003 reflections change systematically as a function of Fe enrichment in the octahedral sheet. The intensity of the 002 reflection increases with increasing Fe, whereas the intensity of the 003 reflection decreases with Fe enrichment. The 004 reflections remain very weak, and the 005 and 006 reflections change little by increasing Fe.

Systematic intensity change of the 00*l* reflections is also observed in hydrated dioctahedral smectites(Fig. 2). The intensity of the 002 reflection decreases gradually with increasing Fe in contrast to that of the 002 reflection in ethylene-glycolated smectites. The 003 reflections are very weak, and the 004 reflections remain relatively strong in hydrated smectites.

Trioctahedral Smectites (Saponite-Iron Saponite Series)

Fe substitution in ethylene-glycolated trioctahedral smectite produces the effects that are observed in XRD patterns of dioctahedral smectites (Fig. 3); the 002 and 003 reflections decrease gradually with increasing Fe. The 004 reflections

are very weak, and the intensities of 005 and 006 reflections change little with Fe enrichment.

The 002 and 003 reflections of hydrated smectites are relatively weak(Fig. 4). The 003 reflection become stronger with increasing Fe. The 002 peaks become weaker with increasing Fe, and they are almost absent in smectites whose octahedral cations are $Mg_{1.5}$ $Fe_{1.5}$ per formula. However, the intensity of the 002 reflections increases with increasing Fe starting from the octahedral composition of approximately $Mg_{1.5}$ $Fe_{1.5}$.

Heterogeneous Smectites

XRD patterns of smectites that are randomly interstratified with smectite layers having different octahedral composition were calculated using the NEWMOD program. The effects of chemical heterogeneity at a unit-cell scale to XRD profile can be investigated by comparing calculated XRD pattern of heterogeneous smectite and that of homogeneous smectite having average composition of the heterogeneous smectite.

Fig. 5a shows the calculated pattern of randomly interstratified beidellite and nontronite having octahedral compositions of $Al_{2.0}Fe_{0.0}$ and $Fe_{1.7}Al_{0.3}$ per formula, respectively. In XRD pattern calculation, the ratio of beidellite and nontronite was set to be 50:50, and they were as-

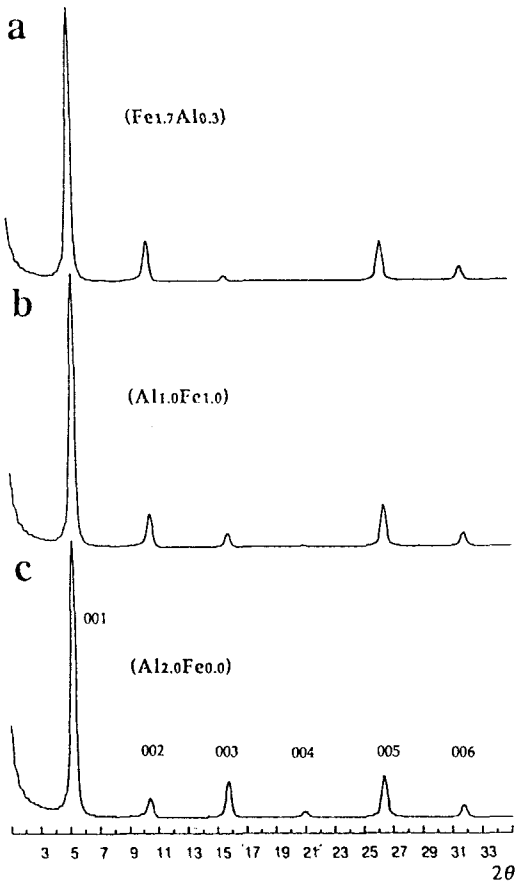

Fig. 1. Calculated XRD patterns (CuKα radiation) of ethylene-glycolated dioctahedral smectites having octahedral Fe of (a) 0, (b) 1.0, and (c) 1.7 per formula. N = 3 to 14.

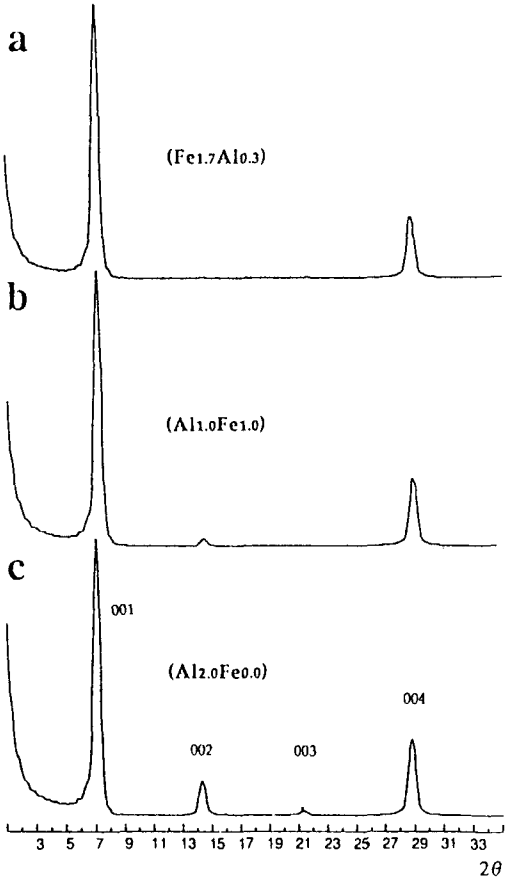

Fig. 2. Calculated XRD patterns (CuKα radiation) of 1-water layer dioctahedral smectites having octahedral Fe of (a) 0, (b) 1.5, and (c) 3.0 per formula. N = 3 to 14.

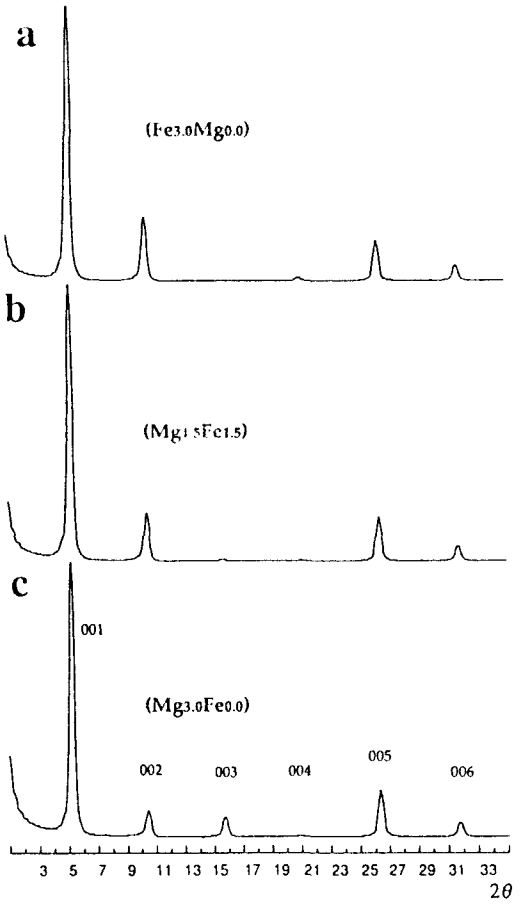

Fig. 3. Calculated XRD patterns (CuKα radiation) of ethylene-glycolated trioctahedral smectites having octahedral Fe of (a) 0, (b) 1.5, and (c) 3.0 per formula. $N = 3$ to 14.

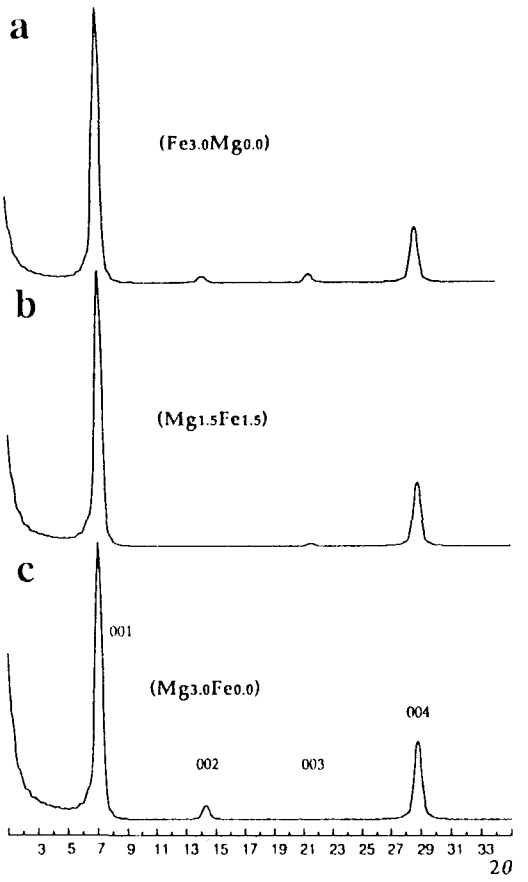

Fig. 4. Calculated XRD patterns (CuKα radition) of 1-water layer trioctahedral smectites having octahedral Fe of (a) 0, (b) 1.5, and (c) 3.0 per formula. $N = 3$ to 14.

sumed to be randomly interstratified (R = 0). The calculation results showed that there is little difference between the XRD patterns of heterogeneous smectite and homogeneous one whose octahedral composition is $Al_{1.15}Fe_{0.85}$ per formula (Fig. 5b). No significant difference between heterogeneous and homogeneous smectites was observed in the calculated XRD patterns of trioctahedral smectite (Fig. 6).

THE EFFECT OF CHEMISTRY ON INTENSITY

The intensity of XRD patterns can be calculated by taking the products of the interference function Φ, the layer scattering intensity G^2, and the Lorentz-polarization factor L_P, at each θ (Reynolds, 1980; Moore and Reynolds, 1989),

$$I(\theta) = [G^2(\theta)]\,[\Phi(\theta)]\,[L_P(\theta)]. \quad (1)$$

Lorentz-polarization factor L_P is a function of θ, and it is not affected by the structure and chemistry of minerals. The polarization factor accounts for the increase in peak and background internsities at low 2θ. The X-ray tube produces unpolarized X-rays whose polarization is dependent on the angles of the incident and diffracted beam. The total energy of the scattered beam is

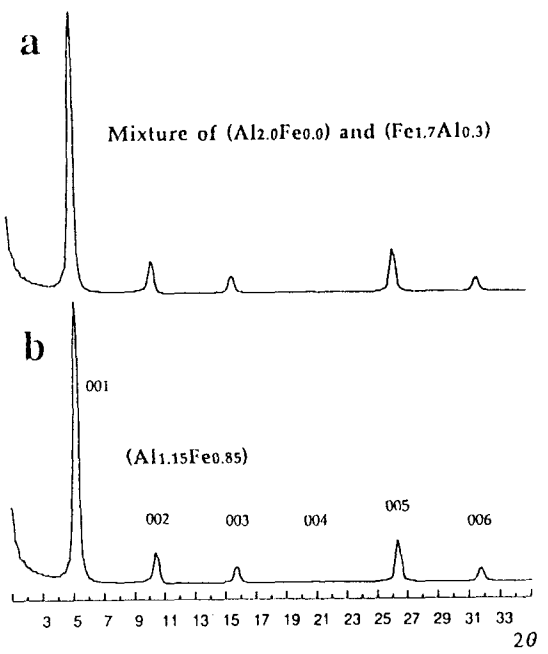

Fig. 5. Calculated XRD patterns (CuKα radiation) of ethylene-glycolated dioctahedral smectites. (a) heterogeneous smectite composed of randomly interstratifed beidellite and nontronite having octahedral compositions of $Al_{2.0}Fe_{0.0}$ and $Fe_{1.7}Al_{0.3}$ per formula, respectively. (b) pure ferrous dioctahedral smectite having octahedral composition of $Al_{1.15}Fe_{0.85}$. N=3 to 14.

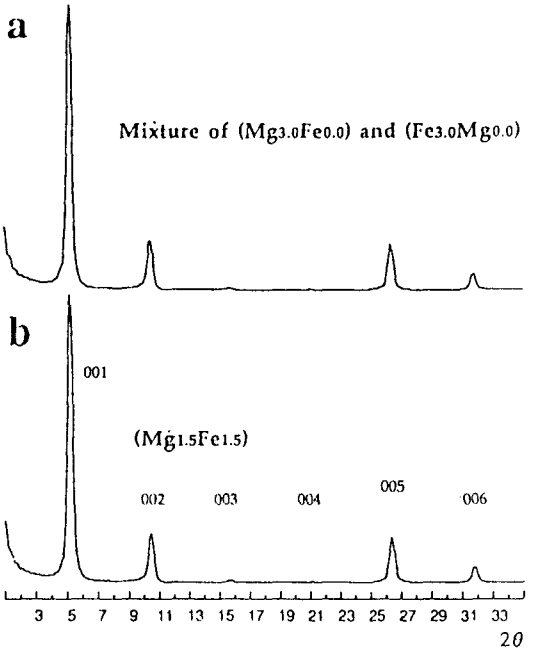

Fig. 6. Calculated XRD patterns (CuKα radiation) of ethylenne-glycolated trioctahedral smectites. (a) heterogeneous smectite composed of randomly interstratified saponite and iron saponite having octahedral compositions of $Mg_{3.0}Fe_{0.0}$ and $Fe_{3.0}Mg_{0.0}$ per formula, respectively. (b) pure ferrous trioctahedral smectite having octahedral composition of $Mg_{1.5}Fe_{1.5}$. N= 3to14.

lost proportional to the factor $(1+\cos^2 2\theta)/2$ where θ is the angle between the incident beam and the reflected plane. The Lorentz factor is related to the volume of the crystals exposed to the X-rays and the number of crystals favorably oriented for diffraction at any Bragg angle. The Lorentz factor for micaceous minerals showing high degree of preferred orientation was discussed by Reynolds (1976).

The Interference function Φ is also needed in calculating XRD pattern profiles of specimens composed of very thin crystals such as clay particles, because additional scattering occurs at 2θ adjacent and even far from the Bragg angles in thin crystals. Φ is a continuous function of θ, and it is expressed as

$$\Phi(\theta) = \frac{\sin^2(2\pi ND\sin\theta/\lambda)}{\sin^2(2\pi D\sin\theta/\lambda)}, \qquad (2)$$

where N is the number of unit cells stacked in coherent scattering array along the z-axis and $D=d(001)$.

The structure factor of an atomic layer is expressed as

$$\begin{aligned} F(00l) &= f_1 e^{i\phi 1} + f_2 e^{i\phi 2} + \cdots + f_n e^{i\phi n} \\ &= \sum_n f_n e^{i\phi n} \\ &= \sum_n f_n \cos\phi + i\sum_n f_n \sin\phi \end{aligned} \qquad (3)$$

where f and ϕ are scattering factor and phase angle of each atoms of the unit cell. If the structure is centrosymmetric, the sine series equals

zero and

$$F(00l) = \sum_n f_n \cos\phi_n = \sum_n P_n f_n \cos(2\pi l z_n/c). \quad (4)$$

P_n is the number of atom P per atomic layer, l is the order of the reflection, and z_n is the displacement of the atomic layer from the center of symmetry normal to (00l) plane, and c is the length of the unit-cell axis. Peak positions are insensitive to changes of the structure factor F. However, correct intensities are more complicated, because small changes in atomic positions and variations in atoms will change significantly the structure factor and therefore intensities of some reflections.

The layer scattering factor G is essentially the same as the structure factor F except that it is modified to result in a function that is continuous with respect to θ (see, Reynolds, 1980. Rearranging the Bragg law with the index l gives $l = 2d\sin\theta/\lambda$, and structure factor F can be converted to G, resulting

$$G(\theta) = \sum_n P_n f_n \cos(4\pi Z_n \sin\theta/\lambda), \quad (5)$$

where $Z_n = z_n/c$. $|G^2|$ at any 2θ is the square of the scattered amplitude from a unit cell, [001] of which is oriented parallel to the incident beam.

Substitution of cations does not affect L_p and Φ but G. Equation (5) indicates that the atomic scattering factor, and number of atoms, and atomic coordinates Z_n are major factors in determining G and therefore intensities of XRD reflections. If substitution of cations does not result in significant displacement of atoms in the structure, the changes of atomic scattering factors will largely account for the change of resulting G.

Atomic scattering factors of most atoms common in sheet silicates can be calculated using the polynomial equation (Wright, 1973),

$$f(\mu) = \sum_{n=0}^{4} a_n \left(\frac{1}{1+2\mu^2}\right)^n, \quad (6)$$

where $\mu = 1/d = 2\sin\theta/\lambda$.

Calculation result of atomic scattering factors of major cations in smectite is in Table 4. The effects of temperature on the atomic scattering factor were not considered in the calculation for simplicity. Scattering factors of Si and Al are very similar. Thus, the substitution of Al tetrahedrally coordinated Si will have little effect on the total layer scattering factor. The substitution of Mg for Al will cause only minor changes in G, because scattering factors of Mg and Al are also similar. However, the scattering factor of Fe is much higher than that of Al and Mg, and thus the substitution of Fe for Al and Mg at octahedral sites will cause significant changes in G.

Table 4. Atomic scattering factors of cations for CuKα radiation. The calculation is based on the data by Wright (1973).

Cations	f_0 at 001 (θ=2.61°)	f_0 at 002 (θ=5.23°)	f_0 at 003 (θ=7.87°)	f_0 at 004 (θ=10.51°)
$A^{+1.5}$	11.42	11.17	10.74	10.40
Si^{+2}	11.90	11.67	11.26	10.81
Mg^{+2}	9.97	9.88	9.72	9.52
Fe^{+2}	23.91	23.59	23.01	22.46

DISCUSSION

Dioctahedral and Trioctahedral Smec-tites

The 002 and 003 peaks of ethylene-glycolated smectites are fairly prominent, and those two peaks change gradually in accordance with increasing Fe. However, the 002 and 003 reflections of hydrated specimens are relatively weaker than those of ethylene-glycolated smectites, suggesting that the 002 and 003 reflections of hydrated Fe-rich smectites may not be detectable on the diffraction patterns unless the samples contain significant amount of smectite. The intensity of the 002 reflection of hydrated trioctahedral smectite decrease gradually with increasing Fe substitution, but reverse of such trend occurs starting from the smectite having octahedral composition of approximately $Mg_{1.5}Fe_{1.5}$.

XRD patterns of ethylene-glycolated specimens are more useful than those of hydrated

specimens in obtaining informations about octahedral composition using the 002 and 003 intensities because of the trend of 002 reflection intensity of hydrated trioctahedral smectite and relatively weak intensities of the 002 and 003 reflections of hydrated smectites. Different 00*l* intensity distribution of ethylene-glycolated and hydrated smectites is caused by the change of phase angles (ϕ in Eq.5) as a result of different basal spacings of two types of specimens.

The major difference between XRD patterns of ethylene-glycolated dioctahedral and trioctahedral smectites is that the 003 reflections are very weak or almost absent in trioctahedral smectites whereas the 002 reflections are relatively strong. Such simulation results indicate that the intensities of 002 and 003 reflections are correlated to the scattering power of octahedral cations; the 002 reflection becomes stronger with increasing scattering power of octahedral cations, and the 003 reflection becomes weaker.

The scattering power by various octahedral cations can be analyzed quantitatively by comparing their scattering factors. The scattering by Fe is approximately 2.1 and 2.4 times that of Al and Mg for the atomic scattering factors (Table 4). The ratio for Al ranges from 2.09 for 001 to 2.16 for 004, and the ratio for Mg ranges from 2.40 for 001 to 2.36 for 004. Although model structures that are used for the calculaton do not take into account the possible occurrence of unoccupied sites, the effect of vacancies, denoted by □, can be used in order to compare the scattering powers of smectites having different cations in octahedral sites (Brown and Brindley, 1980). For example, the intensity distributions of end-member smectites having ($Al_{2.0}Fe_{0.0}$) and ($Mg_{3.0}Fe_{0.0}$) in octahedral sites per formula will be similar to those of smectites having ($Fe_{0.95}\square_{1.05}$) and ($Fe_{1.25}\square_{2.75}$) per formula, respectively.

XRD pattern of dioctahedral smectite having ($Fe_{1.7}Al_{0.3}$) in octahedral sites (Fig. 1a) exhibits characteristics of higher scattering by octahedral cations than that trioctahedral smectite having ($Mg_{3.0}$ $Fe_{0.0}$) in octahedral site by showing stronger 002 reflection and weaker 003 reflection. The scattering by ($Fe_{1.7}Al_{0.3}$) can be approximated by ($Fe_{1.84}\square_{1.16}$) and its scattering power is similar to that by ($Mg_{1.99}Fe_{1.01}$). Therefore, the layer scattering factor of some dioctahedral smectite will be within the range of that of trioctahedral smectite species, and 00*l* reflections of some ferrous saponite will be similar to those of nontronite(e.g., Figs. 1a and 3b). Such result indicates that some of ferrous dioctahedral smectites cannot be easily distinguished from trioctahedral smectites directly from 00*l* reflections.

Various interlayer cations also cause changes in 00*l* intensities, but the changes are minor compared to those caused by the substitution of octahedral cations(Fig. 7). The intensity ratio of 002/003 of Na smectite is slightly higher than that of K smectite. Such effect on the 002 and 003 reflections caused by K is similar to the effect on those two reflections caused by Fe enrichment. Therefore, the modification of XRD profile caused by the interlayer cations should also be taken into account when octahedral characteristics is investigated using 00*l* reflections. Such results indicate that the dioctahedral smectites, especially Fe-

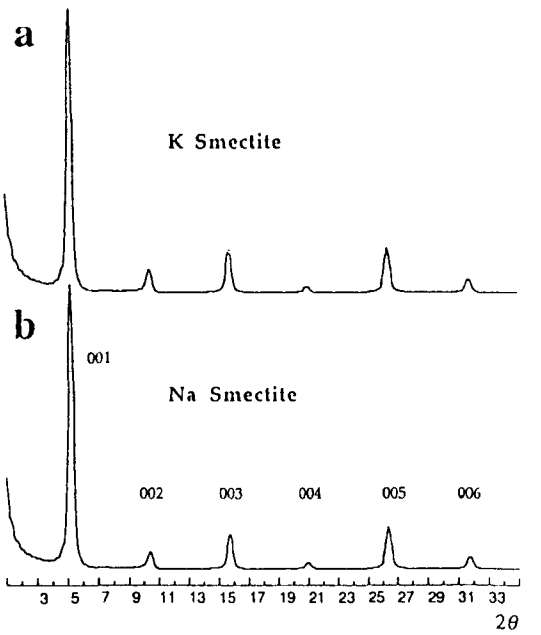

Fig. 7. Calculated XRD patterns (CuKα radiation) of ethylene-glycolated dioctahedral smectites (octahedral composition of $Al_{2.0}Fe_{0.0}$ per formula) whose interlayer cations are (a) K and (b) Na. N=3 to 14.

rich smectites, can be hardly distinguished in practice from trioctahedral smectites because of number of factors affecting the intensity distribution.

The correlation between *c*-dimenion and octahedral cations can be determined in chlorites (Radoslovich, 1962; Baily, 1972), but such correlation is difficcult to be established for smectite series. The basal spacing of ethylene-glycolated smectite may vary depending on the degree of interlayer expansion, and the *d*(001) value of hydrated specimens varies continuously depending on available water or relative humidity (Nagelschmidt, 1936; Bradley et al., 1937). The investigations of synthetic biotites with various proportion of Fe replacing Mg indicate that there is little variation of basal spacings (Wones, 1963; Hewitt and Wones, 1975). However, *b*-dimension is very sensitive to the substitution of octahedral cations (Radoslovich, 1962).

The 060 reflection may used in distinguishing dioctahedral and trioctahedral types, although the peak may be weak because of preferred orientation of clay particles. The length of *b*-axis is more sensitive to the size of octahedral cations and site occupancy in the octahedral sites than that of *a* or *c* dimension. Most dioctahedral and trioctahedral sheet silicates can be identified from 060 reflection using the data by Brindley (1980) and Bailey (1980). However, nontronite (*d*(060)=1.521 Å) and saponite (*d*(060)=1.520 Å) have almost identical values (Brindley, 1980), and these two minerals cannot be unambiguously differentiated without additional data by other analytical methods.

Chemical and X-ray characteristics of dioctahedral Fe-rich smectites were studied by Brigatti (1983), and she obtained a regression equation, $b(\text{Å})\pm0.009=8.893+0.124[\text{total Fe}]$. Brigatti (1983) suggested that the total octahedral occupancy of dioctahedral smectite may not be exactly 2. Furthermore, she suggested that there is not a continuous isomorphous series in smectite group as would be expected on the basis of chemical formula. The presence of smectite whose structural state is intermediate between dioctahedral and trioctahedral state is still unsolved, and possible occurrence of intermediate phases would cause problems in unambiguous identification of dioctahedral smectites from trioctahedral types.

The Effect of Heterogeneity

Simulations showed that heterogeneous smectites result in intense and relatively sharp XRD peaks despite random mixed-layering and compositional variation of component layers (Figs. 5 and 6). Calculation results of mixed-layer I/S by Drits(1987) also showed that XRD profiles are generally not sensitive to the degree of heterogeneity. The similarity of XRD profiles of heterogeneous smectites and homogeneous smectites having average compositions of heterogeneous ones (Figs. 5 and 6) suggests that the degree of heterogeneity of smectites cannot be easily evaluated from XRD profile.

Chemical heterogeneity of component smectite layers may case slightly different basal spacings, and therefore resulting XRD peaks will be slightly broadened. However, the broadening of XRD peaks is also a function of the size of crystal domains (N in Eq. 2) that produce coherent scattering (Reynolds, 1980), and structural defects such as stacking faults will also result in broadening. Therefore, the broadening of 00*l* reflections cannot be used in examining the degree of heterogeneity of the crystals unless other factors affecting the peak broadening are well understood.

CONCLUSIONS

The 002 and 003 reflections of smectite show systematic changes with increasing Fe in octahedral sites. However, these two reflections of hydrated smectites are much weaker that those of ethylene-glycolated smectites, indicating that hydrated specimens may not be useful in obtaining information about the chemistry of octahedral cations. The intensity of the 002 relfection increases with increasing Fe in ethylene-glycolated smectites, but that of the 003 reflection decrease with Fe enrichment. Dioctahedral Fe-rich smectites such as nontronite show XRD charateristics that are similar to that of trioctahedral Mg-rich smectite as a result of relatively high

scattering power of the octahedral sheets, and therefore some dioctahedral smectites cannot be distinguished from triocahedral ones only from 00*l* reflections. The types of interlayer cations do not cause critical effect in determining the intensity distribution of the basal reflections.

Heterogeneous smectites that are composed of randomly interstratified layers having variable compositions show XRD profiles that are almost identical to that of pure smectites having the average composition of heterogeneous ones. This result suggests that the presence of heterogeneous smectites in sediments and soils cannot be unambiguously identified on the basis of the profile of 00*l* reflections.

Acknowledgments : The author wish to thank Drs.J.K.Kang, S.J.Han, and B.K.Park of the Korea Ocean Research and Development Institute (KORDI) for help during the study. This study was supported by the Basic Research Project (PE000221) provided by KORDI and partly by the Deep Seabed Mineral Resources Project (PG00118-2) funded by the Ministry of Science and Technology.

REFERENCES

Ahn, J.H. and Buseck, P.R.(1990) Layer-stacking sequences and structural disorder in mixed-layer illite/smectite: image simulations and HRTEM imaging. Am. Miner., 75, 267-275.

Ahn, J.H. and Peacor, D.R.(1986) Transmission and analytical electron microscopic study of diagenetic chlorite in Gulf Coast argillaceous sediments. Clays Clay Miner., 34, 165-179.

Altaner, S.P. and Bethke, C.M.(1988) Interlayer order in illite/smectite. Am. Miner., 73, 766-774.

Bailey, S.W. (1972) Determination of chlorite compositions by X-ray spacings and intensities. Clays Clay Miner., 20, 381-388.

Bailey, S.W.(1980) Structure of layer silicates. In: Brindley, G.W. and Brown, G.(Eds.) Crystal Structures of Clay Minerals and Their X-ray Identification Miner. Soc. London, 1-123.

Bethke, C.M. and Reynolds, R.C.(1986) Recursive method for determining frequency factors in interstratified clay diffraction calculations. Clays Clay Miner., 34, 224-226.

Bradley, W.F., Grim, R.E. and Clark, G.F.(1937) A study of the behavior of montmorillonite on wetting. Z. Kristallogr., 97, 260-270.

Brigatti, M.F.(1983) Relationships between composition and structure in Fe-rich smectites. Clay Miner., 18, 177-186.

Brindley, G.W.(1980) Order-disorder in clay mineral structure. In: Brindley, G.W. and Brown, G.(Eds.) Crystal Structures of Clay Minerals and Their X-ray Identification. Miner. Soc. London, 125-195.

Brown, G., and Brindley, G.W.(1980) X-ray diffraction procedures for clay mineral identification. In: Brindley, G.W. and Brown, G.(Eds.) Crystal Structures of Clay Minerals and Their X-ray Identification. Miner. Soc. London, 305-359.

Drits, V.A.(1987) Mixed-layer minerals: diffraction methods and structural features. In: Schultz L.G., van Olphen, H. and Mumpton F. A.(Eds.) Proceedings of the International Clay Conference, Denver, 1985. The Clay Minerals Society, 33-45.

Güven, N.(1988) Smectites. In: S.W.Bailey(Ed.) Hydrous Phyllosilicates, Reviews in Mineralogy, 19, 497-559.

Hewitt, D.N. and Wones, D.R.(1975) Physical properties of some synthetic Fe-Mg-Al trioctahedral biotites. Am. Miner., 60, 854-862.

Hower, J., Eslinger, E., Hower, M.E. and Perry, E. A.C1976) Mechanism of burial metamorphism of argillaceous sediments: 1. Mineralogical and chemical evidence. Geol. Soc. Amer. Bull., 87, 725-737.

Moore, D.M. and Reynolds, R.C.(1989) X-ray Diffraction and the Identification and Analysis of Clay Minerals. Oxford Univ. Press, Oxford, 332p.

Nadeau, P.H., Tait, J.M., McHardy, W.J.and Wilson, M.J.(1984a) Interstratified XRD characteristics of physical mixtures of elementary clay particles. Clay Miner., 19, 67-76.

Nadeau, P.H., Wilson, M.J., McHardy, W.J. and Tait, J.M.(1984b) Interstratified clays as fundamental particles. Science, 225, 67-76.

Nagelschmidt, G.(1936) The nature of montmoril-

lonite. Z. Kristallogr., 93, 481-487.

Perry, E. and Hower, J.(1970) Burial diagenesis in Gulf Coast pelitic sediments. Clays Clay Miner, 18, 165-177.

Radoslovich, E.W.(1962) Cell dimensions and symmetry of layer-lattice silicates. Am. Miner., 47, 617-636.

Reynolds, R.C.(1965) An X-ray study of an ethylene glycol-montmorillonite complex. Am. Miner., 50, 990-1001.

Reynolds, R.C.(1967) Interstratified clay systems: calculation of the total one-dimensional diffraction function. Am. Miner., 52, 661-672.

Reynolds, R.C.(1976) The Lorentz factor for basal reflections from micaceous minerals in oriented powder aggregates. Am. Miner., 61, 484-491.

Reynolds, R.C.(1980) Interstratified Clay Minerals. In: Brindley, G.W. and Brown, G.(Eds.) Crystal Structures of Clay Minerals and Their X-ray Identification. Miner. Soc. London. 249-303.

Reynolds. R.C.(1985) NEWMOD® a Computer Program for the Calculation of One-Dimensional Diffraction Patterns of Mixed-Layered Clays. R.c. Reynolds, 8 Brook Dr., Hanover, New Hampshire.

Reynolds, R.C. and Hower, J.(1970) The nature of interlayering in mixed-layer illite/montmorillonite. Clays Clay Miner., 18, 25-36.

Wones, D.R.(1963) Physical properties of synthetic biotites in the join phlogopite-annite. Am. Miner, 48, 1300-1321.

Wright, A.C.(1973) A compact representation for atomic scattering factors. Clays Clay Miner., 21, 489-490.